AGU PUBLICATIONS

Geophysical Research Letters

RESEARCH LETTER
10.1002/2014GL059770

Key Points:
- Greenland contributed up to 6 m equivalent sea level rise during the Pliocene
- Greenland is highly sensitive to Arctic Ocean and sea ice conditions
- Under peak Pliocene warmth, ice sheet retreat is irreversible

Correspondence to:
S. J. Koenig,
koenig@geo.umass.edu

Citation:
Koenig, S. J., R. M. DeConto, and D. Pollard (2014), Impact of reduced Arctic sea ice on Greenland ice sheet variability in a warmer than present climate, *Geophys. Res. Lett.*, *41*, 3934–3943, doi:10.1002/2014GL059770.

Received 28 FEB 2014
Accepted 22 MAY 2014
Accepted article online 27 MAY 2014
Published online 13 JUN 2014

Impact of reduced Arctic sea ice on Greenland ice sheet variability in a warmer than present climate

S. J. Koenig[1], R. M. DeConto[1], and D. Pollard[2]

[1]Department of Geosciences, University of Massachusetts Amherst, Amherst, Massachusetts,USA, [2]Earth and Environmental Systems Institute, College of Earth and Mineral Sciences, Pennsylvania State University, University Park, Pennsylvania, USA

Abstract A global climate model with interactive vegetation and a coupled ice sheet-shelf component is used to test the response of the Greenland ice sheet (GIS) to increased sea surface temperatures (SSTs) and reduced sea ice (SI) cover during the mid-Pliocene warm period (~3 Ma) as reconstructed from proxy records. Seasonally open water in the Arctic and North Atlantic are shown to alter regional radiation budgets, storm tracks, and moisture and heat advection into the Greenland interior, with increases in temperature rather than precipitation dominating the ice sheets response. When applied to an initially glaciated Greenland, the presumed warm, ice-free Pliocene ocean conditions induce rapid melting of nearly the entire ice sheet and preclude a modern-like GIS from (re)growing, regardless of orbital forcing. The sensitivity of Greenland to imposed Pliocene ocean conditions may have serious implications for the future response of the ice sheet to continued warming in the Arctic basin.

1. Introduction

Reductions of Arctic sea ice cover and thickness over the last few decades have been correlated with amplified warming at polar latitudes [*Nghiem et al.*, 2007; *Lindsay et al.*, 2009; *Screen et al.*, 2013]. With models predicting a continued negative trend in perennial sea ice, summer Arctic ice-free conditions will likely be reached by the middle to end of the 21st century [*Drobot et al.*, 2006; *Zhang and Walsh*, 2006; *Maslowski et al.*, 2012; *Stroeve et al.*, 2012]. Changes in sea ice (SI) exert strong influences on local and regional climate via feedbacks determining energy and hydrological budgets [*Serreze et al.*, 2005; *Kinnard et al.*, 2008; *Steele et al.*, 2008] which significantly contribute to Arctic temperature amplification [*Serreze et al.*, 2009; *Screen and Simmonds*, 2010; *Overland and Wang*, 2013]. Recent observations of surface melting on the Greenland ice sheet (GIS) as derived from satellite measurements and instrumental data [*Hanna et al.*, 2008; *Bhattacharya et al.*, 2009; *van den Broeke et al.*, 2009; *Hall et al.*, 2013], and climate simulations extending into the future [*Ridley et al.*, 2010; *Rae et al.*, 2012; *Seddik et al.*, 2012; *Fettweis et al.*, 2013], also point to a highly sensitive GIS. However, the potential long-term mass balance response to changing sea ice conditions in a warmer than modern world has yet to be quantified.

The mid-Pliocene warm period (3.29 to 2.97 Ma) has been identified as a potential analog for future climate, because proxy-based climate reconstructions are comparable to the global mean temperatures predicted for the end of the next century [see *Solomon et al.*, 2007; *Haywood et al.*, 2011a]. Maximum Pliocene sea levels remain poorly constrained [*Raymo et al.*, 2011], but some estimates are several tens of meters higher than today implying the loss of Greenland and some Antarctic glacial ice. A comprehensive multiproxy data set for the Pliocene shows higher than modern sea surface temperatures (SSTs) and an Arctic Ocean free of summer sea ice, while most boundary conditions, including pCO_2, were similar to modern [*Dowsett et al.*, 2010]. Modeled circum-Arctic terrestrial temperatures have been shown to be sensitive to Pliocene sea ice extent [*Ballantyne et al.*, 2013] in keeping with proxy summer temperature reconstructions [*Brigham-Grette et al.*, 2013], but the response of the GIS to sea ice forcing has not been tested. While mid-Pliocene SSTs are reasonably well constrained, the extent, size, and variability of the GIS during this time cannot be determined by available proxies [*Polyak et al.*, 2010] and continues to be debated in modeling studies [*Lunt et al.*, 2009; *Hill et al.*, 2010; *Dolan et al.*, 2011; *Koenig et al.*, 2011].

Guided by proxy ocean reconstructions, we use a global climate model (GCM) with interactive vegetation and a coupled 3-D ice sheet component, to quantify the sensitivity of the GIS to the combined effect of imposed Pliocene SSTs and SI. Simulations are initialized with either a modern ice sheet or an ice-free

Greenland in order to test (1) the response of an existing ice sheet to warm Pliocene ocean conditions and (2) the potential regrowth of ice on Greenland after deglaciation. Our climate analysis focuses on the atmospheric transport of Greenland-bound heat and moisture, in order to understand the role of SSTs and SI in past GIS variability.

2. Methods

2.1. Experimental Design, Proxy Data Set, and Model Setup

We use the latest (2012) version of the Global Environmental and Ecological Simulation of Interactive Systems 3.0 GCM [*Thompson and Pollard*, 1997; *Alder et al.*, 2011] with an interactive vegetation component (Equilibrium Biogeography-Biogeochemistry Model BIOME4) [*Kaplan et al.*, 2003] and a coupled thermomechanical 3-D ice sheet/shelf model [*Pollard and DeConto*, 2012]. The GCM has coupled components of the atmosphere, surface mixed-layer ocean, vegetation, snow, soil, and sea ice, and its performance in polar latitudes has been studied extensively [*DeConto et al.*, 2007].

We quantify and isolate the SST/SI-forcing by contrasting the effects of present-day *Shea et al.* [1991] versus Pliocene ocean conditions, while keeping orbital parameters the same as modern and pCO_2 (405 ppmv) forcings unchanged [see also *Haywood et al.*, 2011b]. Warm Pliocene monthly SSTs and SI fractional cover are provided by the latest (Pliocene Research, Interpretation and Synoptic Mapping (PRISM) 3D Reconstruction) data set of the U.S. Geological Survey PRISM project [*Dowsett et al.*, 2010, and references therein]. The prescribed and fixed Pliocene ocean conditions replace the prognostic ocean component of the model and are implemented into the GCM following the methods established for the Pliocene Model Intercomparison Project (PlioMIP) [*Haywood et al.*, 2011b; *Koenig et al.*, 2012].

PRISM3 includes the most complete ocean data set for the mid-Piacenzian warm period, representing time-averaged conditions between ~3.29 and 2.97 Ma. As in any proxy-based climate reconstruction, uncertainties in the PRISM3 ocean climatology remain [*Dowsett et al.*, 2010; *Hill et al.*, 2010]; however, the reconstruction provides an important standard for the modeling community, and it has been used extensively in model intercomparisons and data synthesis analyses [see *Haywood et al.*, 2011a; *Fedorov et al.*, 2013]. Importantly, reconstructed Pliocene annual SSTs in the North Atlantic and Nordic seas are 6 to >12°C warmer than present and are accompanied by large spatial changes in seasonal sea ice cover. Arctic Ocean warmth is less pronounced relative to modern conditions, but reconstructed summer sea ice is nonexistent during peak Pliocene warmth [see also *Robinson et al.*, 2008; *Robinson*, 2009; *Polyak et al.*, 2010]. In this case, we assume the PRISM3 ocean climatology is valid despite possible uncertainties in the data.

The interactive equilibrium biogeography-biogeochemistry model, BIOME4 [*Kaplan et al.*, 2003], is coupled to the GCM following *Koenig et al.* [2011], to predict global equilibrium vegetation distribution (27 biomes) in response to imposed forcings and feedbacks. We initialize the model with bare ground and equilibrium is reached after ~25 years of integration. Differences in biome patterns can be attributed to SST/SI feedbacks, which alter precipitation and temperature patterns enough to change Arctic distributions of cold deciduous and evergreen forest in lower elevations, while reducing areal extents of tundra in higher elevations (not shown).

The Penn State/UMass 3-D thermomechanical ice sheet-shelf model [*Pollard and DeConto*, 2012] is adapted to Greenland and coupled to the GCM, with ice-driving climatologies calculated from the last 10 years of equilibrated 35 year climate simulations, to minimize biases introduced by interannual variability. The ice sheet model (ISM) is run on a latitude-longitude grid, with a nominal resolution of $0.125° \times 0.25°$. The GCM climatological fields are downscaled to the finer ISM grid using lapse rate corrections to account for the offsets between the GCM and local ice surface elevations [*Pollard and Thompson*, 1997]. A standard Positive Degree Day scheme [*DeConto and Pollard*, 2003] is used to calculate ablation on snow and firn versus ice, while accounting for runoff, refreezing, and percolation of meltwater. For this study no marine ice (floating ice shelves or advance into ocean) is allowed, as is reasonable for modern and smaller Greenland configurations. Ice sheet simulations are initialized either with (i) a present-day ice sheet configuration from a previous model simulation driven by a modern observed climatology [see also *Koenig et al.*, 2011] with 2.81×10^6 km^3 in volume and 1.7×10^6 km^2 in extent, slightly smaller than the observed current volume of 2.96×10^6 km^3 [*Bamber et al.*, 2013], or (ii) ice-free Greenland, with land surface elevations based on a 10 min subglacial topography interpolated from a 1 min ice-free orography (ETOPO1) [*Amante and Eakins*, 2009], and rebounded to isostatic equilibrium [*Crucifix et al.*, 2001]. All ice sheet simulations are run beyond

Table 1. Experimental Setup of Model Boundary Conditions and Forcings[a]

Run ID	SST/SI	GIS	pCO_2	Orbits	Vegetation
$PD_{fullice}$	Modern	Modern	405	Modern	Interactive
$PLIO_{fullice}$	PRISM3	Modern	405	Modern	Interactive
$PD_{icefree}$	Modern	Ice-free	405	Modern	Interactive
$PLIO_{icefree}$	PRISM3	Ice-free	405	Modern	Interactive

[a]SST and fractional SI conditions in the GCM are prescribed and fixed from modern [*Shea et al.*, 1991] or PRISM3 [*Dowsett et al.*, 2010] data sets. GIS configurations are modern [*Bamber et al.*, 2001] or ice-free with isostatically rebounded topography. Atmospheric pCO_2 mixing ratios and orbital parameters are held constant. Vegetation is run in interactive mode and responds freely to the imposed forcings and related feedbacks.

equilibrium to 30 kyr. Table 1 summarizes the complete set of model simulations, relevant boundary conditions, and inputs.

2.2. Heat and Moisture Calculations

Source regions of heat and moisture advected into Greenland are relevant for understanding the ice sheet mass balance response to forcing. Net heat sources can be identified by calculating net heat flux into the atmosphere (F_{net}, W m^{-2}) emitted from the ocean defined by

$$F_{net} = L_h + S_h + \mathrm{LW} - \mathrm{SW} \tag{1}$$

where L_h and S_h are latent and sensible heat fluxes and *LW* and *SW* are the net upward longwave and downward shortwave radiative fluxes at the surface. F_{net} is affected by both seasonally released heat into the atmosphere and heat convergence and divergence through transport of prevailing winds. Moisture source regions are defined as maxima of vertically integrated moisture flux divergence, i.e., evaporation minus precipitation ($E - P$) [*Trenberth and Guillemot*, 1998] and is defined by

$$P - E = -\partial W/\partial t - \nabla \bullet Q \tag{2}$$

where W is precipitable water and Q is the atmospheric moisture transport. In addition to $P - E$ locally, the flux itself is of interest because it contains information on the dynamics of atmospheric circulation patterns that result in the distribution of the moisture budget. Moisture trajectories are calculated by integrating over all pressure (sigma) levels (Lagrangian integration) using

$$Q = 1/g \int_{P_{top}}^{P_{surf}} q\, v\, \mathrm{d}p \tag{3}$$

where g is gravity constant, q specific humidity, and v the horizontal wind vector [*Cullather et al.*, 1998, 2000]

3. Results

3.1. Seasonality and Magnitude of Forcing and Response

The seasonality and magnitude of Greenland's response to warm Pliocene ocean conditions is in phase with the seasonal cycle of the net surface oceanic energy balance, with a lag relative to maximum differences in sea ice cover (Figure 1a). Relative to modern conditions, reconstructed sea ice concentrations in the Pliocene (> 60°N) are reduced by 80% in middle to late summer and are ice-free from July to September. The increased open water reduces albedo, increasing the seasonal storage of incoming shortwave radiation (negative downward) with maximum uptake during June–July (Δ30 W m^{-2}). Net outgoing longwave (positive upward) flux is near zero, with the seasonal maximum occurring during boreal winter, but with a less pronounced seasonal dependence. Maximum upward turbulent heat flux of 40–50 W m^{-2} occurs in late fall and winter months when the contrast of atmosphere and underlying ice/ocean temperatures is greatest. Resulting winter temperature differences on Greenland average +10°C, followed by positive summer temperatures of +3°C, with generally higher anomalies in northern Greenland (Figure 1b). Precipitation increases during Pliocene winter months by +30 to 40%, with no significant changes in summer.

Ice sheet mass balance is primarily a function of summer melting. Hence, the persistence of above freezing surface air temperatures is indicative of a potential melt threshold (Figure 1c). Combined elevation and albedo feedbacks generated by the absence of a GIS exerts strong local effects, with maximum temperature anomalies in summer and late fall (8–10°C). As a result, above freezing temperatures with modern ocean

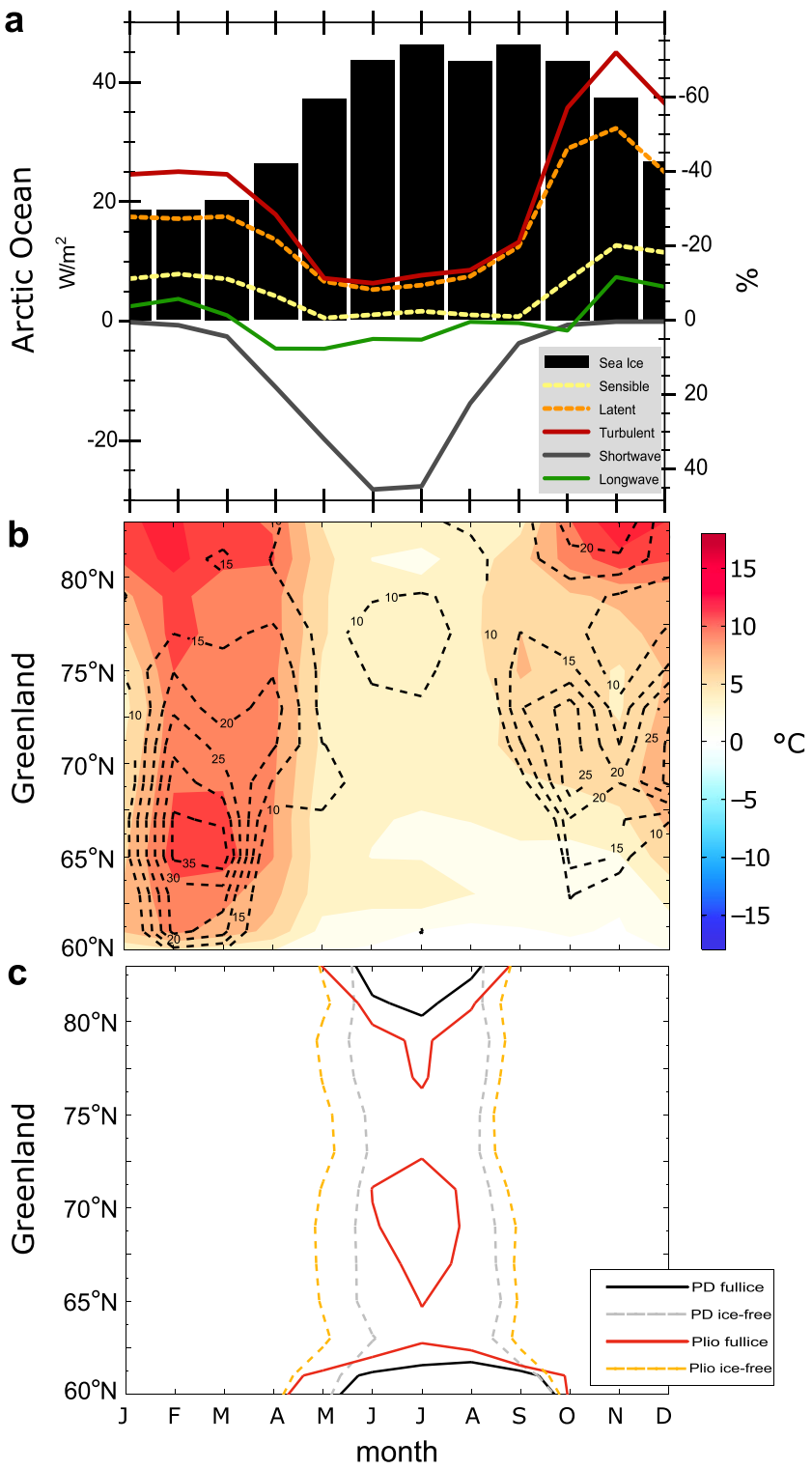

Figure 1. Climatological response to SST/SI forcing. (a) Pliocene sea ice (%) anomalies (black bars) with respect to modern (inversed axis) have an effect on heat fluxes (W m^{-2}, lines) in the Arctic Ocean > 60°N, with positive values of heat directed upward and made available for transport. (b) Seasonal cycle of Pliocene minus present-day surface (2-m) air temperature (filled contours) and precipitation (positive values only, dashed) averaged over a glaciated Greenland. (c) Spatial (latitudinal) and temporal distributions of above freezing temperatures on Greenland for present-day (solid black) and Pliocene glaciated (solid red), and present-day (dashed gray) and Pliocene ice-free (dashed orange) scenarios.

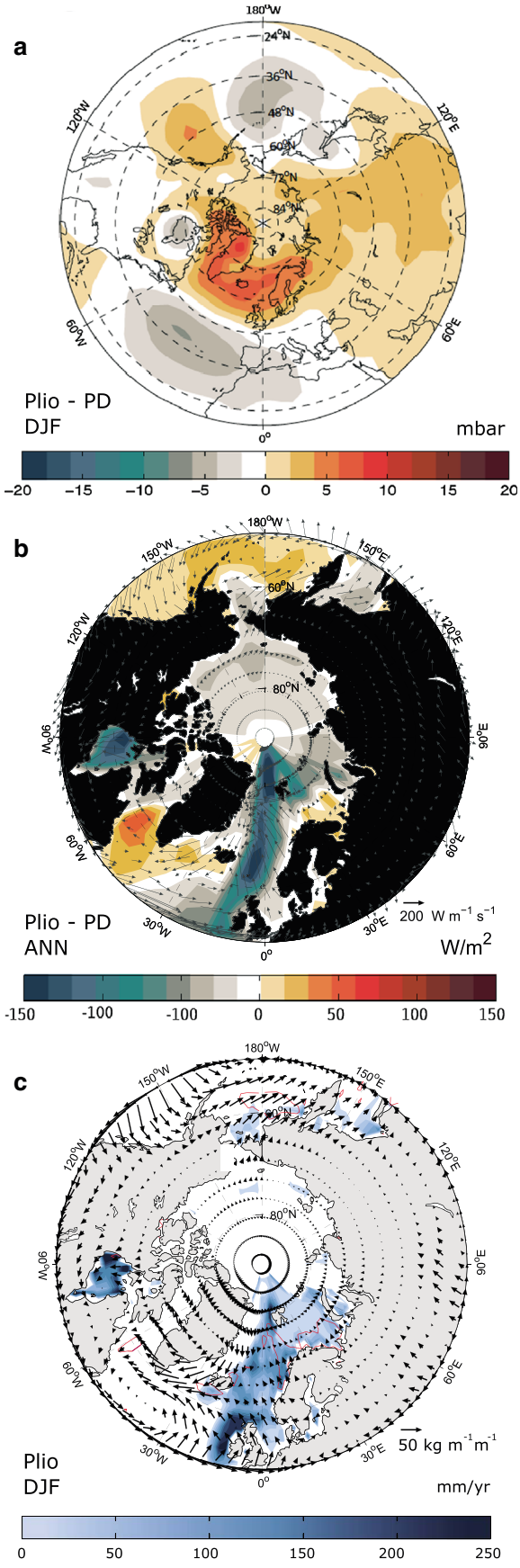

forcing are widespread during May through September on an ice-free Greenland. On a glaciated Greenland, melt is restricted to June–August and only in localized areas in the south and north. Pliocene SST/SI forcing substantially increases the number of positive degree days, with temperatures > 0°C extending into spring and fall on lower elevations and coastal areas, and into the interior of the ice sheet.

3.2. Dynamics

Here we quantify the impact of the SST/SI forcing on Greenland from a hysteresis point of view. Model results are shown that intercompare glaciated scenarios (or ice-free states) with each other. We report on the analysis of Pliocene and modern glaciated simulations before documenting changes between ice-free scenarios.

3.2.1. Atmospheric Pressure

Alternating troughs and ridges define the Arctic sea level pressure system, and altered dynamics act in concert with local and distant ocean conditions to define Greenland-bound transports of heat and moisture. In scenarios with a glaciated Greenland, Arctic winter pressure systems are strongly influenced by the warm Pliocene SSTs and reduced sea ice, even though sea ice differences are greatest during summer. A Student's *t* test reveals that the most significant surface pressure anomalies are simulated over the Atlantic. A weakened and southwardly displaced Icelandic Low of 15 mbar is accompanied by a decrease in the strength of the Azores High and an upper-level ridge response over the

Figure 2. Lower-level atmospheric dynamics and Arctic heat and moisture sources and transports in a glaciated Pliocene versus present-day simulation. (a) Sea level pressure differences (mbar) in December–February (DJF), with tendencies toward a negative mode of the NAO/AO and reduced westerly wind speeds. (b) Differences in net annual surface heat flux F_{net} (W m^{-2}) (negative values upward, filled contours) show heat sources and sinks and show an increase in available heat in the North Atlantic. Heat trajectories (W m^{-1} s^{-1}) in the Pliocene scenario show transport paths from the ocean to Greenland. (c) Absolute surface evaporation minus precipitation $E - P$ (mm yr^{-1}) for the Pliocene (filled blue contours) and present-day (maximum extent, solid red) scenarios. Column-integrated moisture transport (kg m^{-1}s^{-1}) for the Pliocene (DJF) show preferred moisture trajectories and locations of increased precipitation over Greenland.

Arctic (500 hPa, not shown) that reflects a tendency toward a more negative-like North Atlantic/Arctic Oscillation (NAO/AO). Interactions between sea ice and the North Atlantic atmosphere tend to reduce the anomalous pressure pattern through a negative feedback. A diminished North Atlantic meridional temperature gradient accompanies the altered surface pressure field, increasing southerly flow into the Arctic during winter (Figure 1a). In scenarios with no GIS, combined elevation and albedo feedbacks lead to a significantly different atmospheric pressure configuration when compared to the glaciated simulations. As a result, Greenland-bound winds are limited in both deglaciated scenarios, even when warm Pliocene ocean conditions are imposed.

3.2.2. Heat Sources and Transport

The North Atlantic serves as Greenland's main heat source. Differences between Pliocene and modern sea ice produce annual upward heat flux anomalies of 80–150 W m^{-2}. These net positive heat fluxes are most dominant in winter leading to strong diabatic warming over open water. This has an important effect on the atmospheric pressure patterns described above, which in turn have an important effect on the moisture and heat transported to Greenland.

Annual turbulent heat flux trajectories are computed for the lowest level of the model atmosphere (Figure 2b). Relative to modern, Pliocene SST/SI conditions cause 300–400 W m^{-2} of Arctic-bound heat to be diverted into northern Greenland. The heat is transported anticyclonically along the eastern margin of Greenland and into the Irminger Basin and Labrador Sea. The Greenland Sea and Irminger Basin lose less heat in winter, resulting in net positive annual heat gain. In addition, cyclonic geostrophic winds increase heat transport from the Atlantic directly into Greenland. No significant transport to the center of the ice sheet is observed during summer, even though adjacent ocean areas transfer more energy into the atmosphere in that season. The enhanced coastal heat uptake raises surface air temperatures along the Greenland margin. Mean annual temperature differences are as high as +6°C in the center and west of Greenland and +12°C along the eastern and northern coasts. When the ice sheet is removed, heat transport to Greenland is reduced due to the dynamical effects described above. Temperature anomalies mirror local surface characteristics, i.e., vegetation, which determine the local partitioning of sensible and latent heating. As a result, annual temperatures are 7–8°C higher on an ice-free Greenland with the imposed warm Pliocene ocean and sea ice conditions (see Figure 1b).

3.2.3. Moisture Sources and Transport

Moisture sources are closely related to latent heat flux from the ocean or land, defining specific humidity available for transport (Figure 2c). Present-day sources (areas of negative $P - E$) of potential oceanic moisture convergence over Greenland are identified along the Norwegian coast, however, they are mostly restricted to winter and spring. Higher mid-Pliocene SSTs and reduced sea ice produce extensive areas of North Atlantic moisture source regions throughout the year. Maximum annual values reach 400 mm yr^{-1} in some locations. Through evaporative processes on vegetated land areas, the Canadian Arctic and northwest Eurasia become terrestrial moisture sources in late spring and summer. These terrestrial sources are similar in present-day and Pliocene simulations. The Arctic Ocean does not provide a significant source of moisture as defined by the $P - E$ budget. In both present-day and Pliocene ice-free scenarios, evaporation on Greenland increases in summer, balancing dynamically driven drying (not shown) and creating an additional local moisture source.

Greenland-bound moisture is determined by available humidity and the prevailing wind patterns in the North Atlantic, with limited influence from the Arctic Ocean (Figure 2c). Moisture transport is mostly driven by low-level winds from the Nordic Seas toward the eastern Greenland margin, followed by anticyclonic flow toward the western and northern margins (20 kg $m^{-1}s^{-1}$). This moisture flow is enhanced by water vapor advected northward into the Irminger Basin and Labrador Sea through a weakened Icelandic Low. In summer, prevailing winds inhibit moisture transport to the ice sheet. This holds true both in present-day and Pliocene simulations. The Atlantic precipitation signal in winter mirrors the tendency toward the negative NAO pattern described above. Annual $P - E$ follows the patterns of moisture sources and trajectories over the ocean, with negative values of 0.5–4 mm yr^{-2} and net positive precipitation anomalies over Greenland's eastern coastal areas. Although some moisture is precipitated locally within the moisture source regions, significant transport into Greenland occurs during winter (60 kg m^{-1} s^{-1}). Importantly, the prevailing winds in the scenarios with no ice sheet limit moisture transport into Greenland, even when source areas are enhanced with warm Pliocene ocean and sea ice conditions. The annual net precipitable water over an ice-free Greenland is primarily controlled by local land surface characteristics (vegetation distribution and

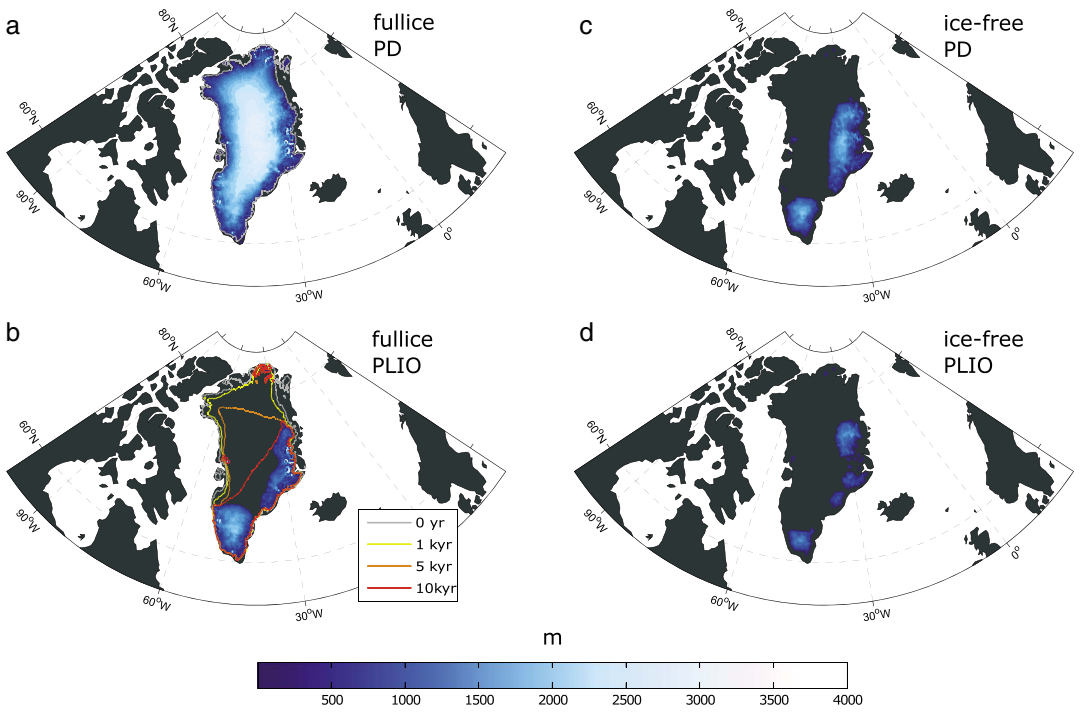

Figure 3. The GIS response to Pliocene SST/SI conditions. The ice sheet model is run to equilibrium with (a, c) present-day and (b, d) Pliocene forcing (see also Table 1). Starting conditions use a present-day glaciated as shown in Figures 3a and 3b or ice-free, isostatically rebounded Greenland as shown in Figures 3c and 3d. Ice sheet thicknesses (m) are shown after 30 kyr with ice margin extents in Figure 3b shown after 0 year (gray), 1 kyr (yellow), 5 kyr (orange), and 10 kyr (red).

topography), as mirrored in the net $P - E$ pattern and is not significantly different between Pliocene and present-day ocean conditions.

3.3. Cryospheric Response

The effects of warm Pliocene SSTs and reduced sea ice cover on temperature and precipitation have an important effect on ice sheet mass balance. Whereas cold season snow accumulation across much of the Arctic is generally increased with warm Pliocene ocean conditions, average snow depths on a glaciated Greenland are substantially diminished as a result of warming through the dynamical heat transport described above. Statistically significant differences in snow thickness on the ice sheet margins simulated by the GCM are on the order of $>$ 10 m. August snow height is reduced from the ice edges, upslope into the interior of the ice sheet, following the 0°C and −10°C isotherms. On an ice-free Greenland, the net effect of Pliocene ocean conditions is to increase spring snow thickness in March, but the net effect of annual warming reduces snow budgets in higher elevations.

To assess the sensitivity of the GIS to warmer Pliocene SSTs and reduced sea ice cover, the ice sheet model was run with the different climatologies described above (Figure 3). Initializing the ISM from a modern ice-sheet geometry (Figures 3a and 3b, gray lines) and driving the ISM with a GCM climatology with modern prescribed SSTs produces no significant change in the ice sheet, even with slightly elevated Pliocene pCO_2 (405 ppm). In contrast, prescribing the reconstructed Pliocene SST/SI conditions in the GCM diminishes the ice sheet by 71% in extent and 83% in volume, corresponding to an equivalent sea level rise of 5.8 m. The melting starts at lower elevations in the north, with the terrestrial ice-sheet margin retreating southward to the highest elevations in the southeast. Most of the ice sheet retreat occurs within the first 5000 year (1.24×10^6 km^2, 2.02×10^6 km^3), with melting rates of up to 150 m^2 yr^{-1} year at year 1 to year 1000 of the integration before equilibrating at approximately 12 kyr. While orbital parameters in these simulations are held at modern values, the timescale of the retreat is within a precession cycle. Adding the effect of warm austral summer orbits would accelerate the pace and magnitude of retreat, making these results conservative within the broader context of mid-Pliocene climate.

Ice sheet simulations initiated over ice-free rebounded topography test the potential for the regrowth of ice caps on a deglaciated Greenland, under both modern and Pliocene conditions (Figures 3c and 3d). Under a Pliocene climatology, equilibrated ice caps are limited to the highest elevations (900–1500 m) in southern and eastern Greenland. The additional impact of Pliocene SST/SI conditions result in smaller ice caps with a sea level equivalent volume of only 0.27×10^6 km^2 (15% of a present-day ice sheet), 0.24×10^6 km^3 (7.6%), and Δ sea level of +6.46 m compared to modern. The nucleation zones of the ice caps simulated under modern conditions are about twice the extent of those in the warm Pliocene scenarios, but the resulting ice caps are still limited to higher elevations and never coalesce to reform a large ice sheet. This implies that once lost, the GIS would only regrow if pCO_2 levels dropped well below 405 ppmv and orbital parameters were favorable (producing cold boreal summers) as shown in previous modeling studies [e.g., *Lunt et al.*, 2009; *Koenig et al.*, 2011].

4. Discussion

Modeled climate and variability of a Pliocene GIS is strongly tied to the imposed SST/SI forcing in the North Atlantic, in line with findings from proxy reconstructions of sea surface temperatures [*Lawrence et al.*, 2009] linked to the variability of Greenland through the Plio-Pleistocene. Small changes in the sea ice edge in the North Atlantic are capable of redefining temperature and precipitation signals on Greenland [*Li et al.*, 2005], with far reaching effects on circum-Arctic climate [e.g., *Smith et al.*, 2005; *Ballantyne et al.*, 2013]. Greenland-bound heat and moisture from the North Atlantic are ultimately tied to altered pressure patterns in the lower troposphere, with a tendency toward a more permanent negative NAO-like pattern in the Pliocene. A negative NAO has been linked to future projected reductions in sea ice cover at the end of the 21st century [e.g., *Seierstad and Bader*, 2008; *Budikova*, 2009; *Deser et al.*, 2010], in keeping with the results shown here. If the reconstructed Pliocene SSTs in the North Atlantic and Nordic Seas are overestimated, they could be biasing our simulated Greenland climates and ice sheets. Future work should consider the full range of uncertainties in the SST/SI reconstructions used in the GCM [e.g., *Hill et al.*, 2010].

Based on the *Clausius-Clapeyrion* relationship, increases in water vapor and polar precipitation are expected to accompany increasing air temperatures and reduced sea ice cover, making reliable predictions of future ice sheet response difficult. Based on our results (Figures 2 and 3), we conclude that mid-Pliocene cryospheric variability was governed more strongly by temperature than precipitation, in line with other modeling studies for the future [e.g., *Kiilsholm et al.*, 2003; *Huybrechts et al.*, 2011]. The warm Pliocene Greenland temperatures responding to regional SSTs and open water substantially increase summer ablation rates, while modest increases in precipitation are mainly in the liquid fraction. The role of enhanced precipitation on ice sheet inception should be greater for climates closer to the glaciation threshold [e.g., *Sayag et al.*, 2004], i.e., at lower levels of atmospheric pCO_2 and/or colder summer orbital forcing as supported by previous modeling studies of GIS inception [*DeConto et al.*, 2008; *Koenig et al.*, 2011].

The response of the GIS to mid-Pliocene boundary conditions results in near complete deglaciation of Greenland within several thousand years, even with a modern orbital configuration. The warm Pliocene ice sheet is reduced to small ice caps on higher elevations in eastern and southern Greenland, contributing an equivalent of 5.8 to 6.4 m of sea level rise. *Stone et al.* [2010] simulate future loss of ice from Greenland in response to anticipated future warming at atmospheric pCO_2 concentrations between 400 and 560 ppmv. Given 405 ppmv pCO_2 used in this study, the combined effects of warm Pliocene SSTs and reduced sea ice act in combination with other feedbacks, such as vegetation [*Koenig et al.*, 2011], to produce major changes in Greenland's mass balance. Once the ice sheet is lost, regrowth is irreversible under both Pliocene forcings (warmer, more precipitation) and present-day (colder, dryer) scenarios, even when sea surface temperatures and sea ice conditions are prescribed with modern values. Irreversible loss of the GIS has been noted in other modeling studies [see *Ridley et al.*, 2010]. We find this is partly driven by the dynamical effects described above and related shifts in moisture convergence, in addition to local height-mass balance feedback on ablation rates in the relatively low-lying Greenland interior.

Possible model dependency and uncertainties in the imposed sea surface boundary conditions preclude definitive conclusions regarding the precise response of the GIS to Pliocene warmth. Nonetheless, we suggest the demonstrated sensitivity of the GIS to Pliocene forcing, enhanced by the internal feedbacks and dynamical processes discussed here, has important implications for the long-term future of the ice sheet. These results imply that (i) reductions of sea ice and increases of SSTs in the circum-Arctic will lead to a

strongly negative mass balance on Greenland. (ii) The future loss of the ice sheet will be permanent, despite overall increases in North Atlantic precipitation expected to accompany future warming and reductions in Arctic and North Atlantic sea ice.

Acknowledgments
This material is based on work supported by the U.S. National Science Foundation under the awards ATM-0513402, AGS-1203910, and OCE-1202632.

The Editor thanks Harry Dowsett and two anonymous reviewers for their assistance in evaluating this paper.

References

Alder, J. R., S. W. Hostetler, D. Pollard, and A. Schmittner (2011), Evaluation of a present-day climate simulation with a new coupled atmosphere-ocean model GENMOM, *Geosci. Model Dev.*, *4*(1), 69–83, doi:10.5194/gmd-4-69-2011.

Amante, C., and B. W. Eakins (2009), ETOPO1-1 arc-minute global relief model: Procedures, data sources and analysis, *NOAA Technical Memorandum NESDIS NGDC-24*, National Geophysical Data Center, NOAA.

Ballantyne, A. P., Y. Axford, G. H. Miller, B. L. Otto-Bliesner, N. Rosenbloom, and J. W. White (2013), The amplification of Arctic terrestrial surface temperatures by reduced sea-ice extent during the Pliocene, *Palaeogeogr. Palaeoclimatol. Palaeoecol.*, *386*, 59–67.

Bamber, J., S. Ekholm, and W. Krabill (2001), A new, high-resolution digital elevation model of Greenland fully validated with airborne laser altimeter data, *J. Geophys. Res.*, *106*(B4), 6733–6745.

Bamber, J., et al. (2013), A new bed elevation dataset for Greenland, *Cryosphere*, *7*, 499–510, doi:10.5194/tc-7-499-2013.

Bhattacharya, I., K. C. Jezek, L. Wang, and H. Liu (2009), Surface melt area variability of the Greenland ice sheet: 1979–2008, *Geophys. Res. Lett.*, *36*, L20502, doi:10.1029/2009GL039798.

Brigham-Grette, J., et al. (2013), Pliocene warmth, polar amplification, and stepped Pleistocene cooling recorded in NE Arctic Russia, *Science*, *340*(6139), 1421–1427, doi:10.1126/science.1233137.

Budikova, D. (2009), Role of Arctic sea ice in global atmospheric circulation: A review, *Global Planet. Change*, *68*(3), 149–163, doi:10.1016/j.gloplacha.2009.04.001.

Crucifix, M., M. Loutre, K. Lambeck, and A. Berger (2001), Effect of isostatic rebound on modelled ice volume variations during the last 200 kyr, *Earth Planet. Sci. Lett.*, *184*(3–4), 623–633.

Cullather, R. I., D. H. Bromwich, and M. L. Van Woert (1998), Spatial and temporal variability of antarctic precipitation from atmospheric methods, *J. Clim.*, *11*(3), 334–367, doi:10.1175/1520-0442(1998)011<0334:SATVOA>2.0.CO;2.

Cullather, R. I., D. H. Bromwich, and M. C. Serreze (2000), The atmospheric hydrologic cycle over the Arctic basin from reanalyses. Part I: Comparison with observations and previous studies, *J. Clim.*, *13*(5), 923–937, doi:10.1175/1520-0442(2000)013<0923:TAHCOT>2.0.CO;2.

DeConto, R. M., and D. Pollard (2003), Rapid Cenozoic glaciation of Antarctica induced by declining atmospheric CO_2, *Nature*, *10*, 245–249.

DeConto, R. M., D. Pollard, and D. Harwood (2007), Sea ice feedback and Cenozoic evolution of Antarctic climate and ice sheets, *Paleoceanography*, *22*(3), PA3214, doi:10.1029/2006PA001350.

DeConto, R. M., D. Pollard, P. A. Wilson, H. Pälike, C. H. Lear, and M. Pagani (2008), Thresholds for Cenozoic bipolar glaciation, *Nature*, *455*(7213), 652–656.

Deser, C., R. Tomas, M. Alexander, and D. Lawrence (2010), The seasonal atmospheric response to projected Arctic sea ice loss in the late twenty-first century, *J. Clim.*, *23*(2), 333–351, doi:10.1175/2009JCLI3053.1.

Dolan, A. M., A. M. Haywood, D. J. Hill, H. J. Dowsett, S. J. Hunter, D. J. Lunt, and S. J. Pickering (2011), Sensitivity of Pliocene ice sheets to orbital forcing, *Palaeogeogr. Palaeoclimatol. Palaeoecol.*, *309*(1–2), 98–110, doi:10.1016/j.palaeo.2011.03.030.

Dowsett, H., M. Robinson, A. Haywood, U. Salzmann, D. Hill, L. Sohl, M. Chandler, M. Williams, K. Foley, and D. Stoll (2010), The PRISM3D paleoenvironmental reconstruction, *Stratigraphy*, *7*(2–3), 123–139.

Drobot, S. D., J. A. Maslanik, and C. Fowler (2006), A long-range forecast of Arctic summer sea-ice minimum extent, *Geophys. Res. Lett.*, *33*, L10501, doi:10.1029/2006GL026216.

Fedorov, A. V., C. M. Brierley, K. T. Lawrence, Z. Liu, P. S. Dekens, and A. C. Ravelo (2013), Patterns and mechanisms of early Pliocene warmth, *Nature*, *946*, 43–49, doi:10.1038/nature12003.

Fettweis, X., B. Franco, M. Tedesco, J. H. van Angelen, J. T. M. Lenaerts, M. R. van den Broeke, and H. Gallee (2013), Estimating the Greenland ice sheet surface mass balance contribution to future sea level rise using the regional atmospheric climate model MAR, *Cryosphere*, *7*, 469–489, doi:10.5194/tc-7-469-2013.

Hall, D. K., J. C. Comiso, N. E. DiGirolamo, C. A. Shuman, J. E. Box, and L. S. Koenig (2013), Variability in the surface temperature and melt extent of the Greenland ice sheet from MODIS, *Geophys. Res. Lett.*, *40*, 2114–2120, doi:10.1002/grl.50240.

Hanna, E., P. Huybrechts, K. Steffen, J. Cappelen, R. Huff, C. Shuman, T. Irvine-Fynn, S. Wise, and M. Griffiths (2008), Increased runoff from melt from the Greenland ice sheet: A response to global warming, *J. Clim.*, *21*(2), 331–341, doi:10.1175/2007JCLI1964.1.

Haywood, A., A. Ridgwell, D. Lunt, D. Hill, M. Pound, H. Dowsett, A. Dolan, J. Francis, and M. Williams (2011a), Are there pre-Quaternary geological analogues for a future greenhouse warming?, *Philos. Trans. R. Soc. London, Ser. A*, *369*(1938), 933–956.

Haywood, A. M., et al. (2011b), Pliocene model intercomparison project (PlioMIP): Experimental design and boundary conditions (experiment 1), *Geosci. Model Dev.*, *3*, 227–242.

Hill, D., A. Dolan, A. Haywood, S. Hunter, and D. Stoll (2010), Sensitivity of the Greenland ice sheet to Pliocene sea surface temperatures, *Stratigraphy*, *7*(2–3), 111–121.

Huybrechts, P., H. Goelzer, I. Janssens, E. Driesschaert, T. Fichefet, H. Goosse, and M.-F. Loutre (2011), Response of the Greenland and Antarctic ice sheets to multi-millennial greenhouse warming in the Earth system model of intermediate complexity LOVECLIM, *Surv. Geophys.*, *32*, 397–416, doi:10.1007/s10712-011-9131-5.

Kaplan, J. O., et al. (2003), Climate change and Arctic ecosystems: 2. Modeling, paleodata-model comparisons, and future projections, *J. Geophys. Res.*, *108*(D19), 8171, doi:10.1029/2002JD002559.

Kiilsholm, S., J. H. Christensen, K. Dethloff, and A. Rinke (2003), Net accumulation of the Greenland ice sheet: High resolution modeling of climate changes, *Geophys. Res. Lett.*, *30*(9), 1485, doi:10.1029/2002GL015742.

Kinnard, C., C. M. Zdanowicz, R. M. Koerner, and D. A. Fisher (2008), A changing Arctic seasonal ice zone: Observations from 1870–2003 and possible oceanographic consequences, *Geophys. Res. Lett.*, *35*, L02507, doi:10.1029/2007GL032507.

Koenig, S. J., R. M. DeConto, and D. Pollard (2011), Late Pliocene to Pleistocene sensitivity of the Greenland ice sheet in response to external forcing and internal feedbacks, *Clim. Dyn.*, *37*, 1247–1268, doi:10.1007/s00382-011-1050-0.

Koenig, S. J., R. M. Deconto, and D. Pollard (2012), Pliocene Model Intercomparison Project Experiment 1: Implementation strategy and mid-Pliocene global climatology using GENESIS v3.0 GCM, *Geosci. Model Dev.*, *5*, 73–85, doi:10.5194/gmd-5-73-2012.

Lawrence, K. T., T. D. Herbert, C. M. Brown, M. E. Raymo, and A. M. Haywood (2009), High-amplitude variations in North Atlantic sea surface temperature during the Early Pliocene warm period, *Paleoceanography*, *24*(26), PA2218, doi:10.1029/2008PA001669.

Li, C., D. S. Battisti, D. P. Schrag, and E. Tziperman (2005), Abrupt climate shifts in Greenland due to displacements of the sea ice edge, *Geophys. Res. Lett.*, *32*, L19702, doi:10.1029/2005GL023492.
Lindsay, R. W., J. Zhang, A. Schweiger, M. Steele, and H. Stern (2009), Arctic sea ice retreat in 2007 follows thinning trend, *J. Clim.*, *22*(1), 165–176, doi:10.1175/2008JCLI2521.1.
Lunt, D. J., A. M. Haywood, G. L. Foster, and E. J. Stone (2009), The Arctic cryosphere in the mid-Pliocene and the future, *Philos. Trans. R. Soc. London, Ser. A*, *367*(1886), 49–67.
Maslowski, W., J. Clement Kinney, M. Higgins, and A. Roberts (2012), The future of Arctic sea ice, *Annu. Rev. Earth Planet. Sci.*, *40*(1), 625–654, doi:10.1146/annurev-earth-042711-105345.
Nghiem, S. V., I. G. Rigor, D. K. Perovich, P. Clemente-Colon, J. W. Weatherly, and G. Neumann (2007), Rapid reduction of Arctic perennial sea ice, *Geophys. Res. Lett.*, *34*, L19504, doi:10.1029/2007GL031138.
Overland, J. E., and M. Wang (2013), When will the summer Arctic be nearly sea ice free?, *Geophys. Res. Lett.*, *40*, 2097–2101, doi:10.1002/grl.50316.
Pollard, D., and R. M. DeConto (2012), Description of a hybrid ice sheet-shelf model, and application to Antarctica, *Geosci. Model Dev.*, *5*(5), 1273–1295.
Pollard, D., and S. L. Thompson (1997), Climate and ice-sheet mass balance at the last glacial maximum form the GENESIS version 2 global climate model, *Quat. Sci. Rev.*, *16*(96), 841–863.
Polyak, L., et al. (2010), History of sea ice in the Arctic, *Quat. Sci. Rev.*, *29*(15–16), 1757–1778, doi:10.1016/j.quascirev.2010.02.010.
Rae, J. G. L., et al. (2012), Greenland ice sheet surface mass balance: Evaluating simulations and making projections with regional climate models, *Cryosphere Discuss.*, *6*(3), 2059–2113, doi:10.5194/tcd-6-2059-2012.
Raymo, M. E., J. X. Mitrovica, M. J. O'Leary, R. M. DeConto, and P. J. Hearty (2011), Searching for eustasy in Pliocene sea-level records, *Nat. Geosci.*, *4*, 328–332.
Ridley, J., J. M. Gregory, P. Huybrechts, and J. Lowe (2010), Thresholds for irreversible decline of the Greenland ice sheet, *Clim. Dyn.*, *35*(6), 1065–1073, doi:10.1007/s00382-009-0646-0.
Robinson, M. (2009), New quantitative evidence of extreme warmth in the Pliocene Arctic, *Stratigraphy*, *6*(4), 265–275.
Robinson, M. M., H. J. Dowsett, G. S. Dwyer, and K. T. Lawrence (2008), Reevaluation of mid-Pliocene North Atlantic sea surface temperatures, *Paleoceanography*, *23*(3), PA3213, doi:10.1029/2008PA001608.
Sayag, R., E. Tziperman, and M. Ghil (2004), Rapid switch-like sea ice growth and land ice-sea ice hysteresis, *Paleoceanography*, *19*(1), PA1021, doi:10.1029/2003PA000946.
Screen, J. A., and I. Simmonds (2010), The central role of diminishing sea ice in recent Arctic temperature amplification, *Nature*, *464*(7293), 1334–1337, doi:10.1038/nature09051.
Screen, J. A., C. Deser, I. Simmonds, and R. Tomas (2013), Atmospheric impacts of Arctic sea-ice loss, 1979-2009: Separating forced change from atmospheric internal variability, *Clim. Dyn.*, doi:10.1007/s00382-013-1830-9, (to appear in print).
Seddik, H., R. Greve, T. Zwinger, F. Gillet-Chaulet, and O. Gagliardini (2012), Simulations of the Greenland ice sheet 100 years into the future with the full Stokes model Elmer/Ice, *J. Glaciol.*, *58*(209), 427–440, doi:10.3189/2012JoG11J177.
Seierstad, I. A., and J. Bader (2008), Impact of a projected future Arctic Sea Ice reduction on extratropical storminess and the NAO, *Clim. Dyn.*, *33*(7–8), 937–943, doi:10.1007/s00382-008-0463-x.
Serreze, M., A. Barrett, and F. Lo (2005), Northern high-latitude precipitation as depicted by atmospheric reanalyses and satellite retrievals, *Mon. Weather Rev.*, *133*(12), 3407–3430.
Serreze, M., A. Barrett, J. Stroeve, D. Kindig, and M. Holland (2009), The emergence of surface-based Arctic amplification, *Cryosphere*, *3*(1), 11–19.
Shea, D. J., K. E. Trenberth, and R. W. Reynolds (1991), A global monthly sea surface temperature climatology, National Center for Atmospheric Research.
Smith, T. M., T. C. Peterson, J. H. Lawrimore, and R. W. Reynolds (2005), New surface temperature analyses for climate monitoring, *Geophys. Res. Lett.*, *32*, L14712, doi:10.1029/2005GL023402.
Solomon, S., D. Qin, M. Manning, Z. Chen, M. Marquis, K. B. Averyt, M. Tignor, and H. L. Miller (2007), *IPCC, 2007: Climate Change 2007: The Physical Science Basis. Contribution of Working Group I to the Fourth Assessment Report of the Intergovernmental Panel on Climate Change*, Cambridge Univ. Press, Cambridge, U. K.
Steele, M., W. Ermold, and J. Zhang (2008), Arctic Ocean surface warming trends over the past 100 years, *Geophys. Res. Lett.*, *35*, L02614, doi:10.1029/2007GL031651.
Stone, E. J., D. J. Lunt, I. C. Rutt, and E. Hanna (2010), The effect of more realistic forcings and boundary conditions on the modelled geometry and sensitivity of the Greenland ice-sheet. The Cryosphere: An interactive open access journal of the European Geosciences Union, *Cryosphere Discuss.*, *4*, 233–285.
Stroeve, J. C., M. C. Serreze, M. M. Holland, J. E. Kay, J. Malanik, and A. P. Barrett (2012), The Arctics rapidly shrinking sea ice cover: A research synthesis, *Clim. Change*, *110*(3–4), 1005–1027, doi:10.1007/s10584-011-0101-1.
Thompson, S. L., and D. Pollard (1997), Greenland and Antarctic mass balances for present and doubled atmospheric CO_2 from the GENESIS version-2 global climate model, *J. Clim.*, *10*(5), 871–900.
Trenberth, K. E., and C. J. Guillemot (1998), Evaluation of the atmospheric moisture and hydrological cycle in the NCEP/NCAR reanalyses, *Clim. Dyn.*, *14*(3), 213–231, doi:10.1007/s003820050219.
van den Broeke, M., J. Bamber, J. Ettema, E. Rignot, E. Schrama, W. J. van de Berg, E. van Meijgaard, I. Velicogna, and B. Wouters (2009), Partitioning recent Greenland mass loss, *Science*, *326*(5955), 984–986, doi:10.1126/science.1178176.
Zhang, X., and J. E. Walsh (2006), Toward a seasonally ice-covered Arctic Ocean: Scenarios from the IPCC AR4 model simulations, *J. Clim.*, *19*(9), 1730–1747, doi:10.1175/JCLI3767.1.